OPEN ACCESS

Original research

Bacterial biofilms predominate in both acute and chronic human lung infections

Mette Kolpen ,[1] Kasper Nørskov Kragh,[1,2] Juan Barraza Enciso,[3] Daniel Faurholt-Jepsen,[4,5] Birgitte Lindegaard,[5] Gertrud Baunbæk Egelund,[5] Andreas Vestergaard Jensen,[5] Pernille Ravn,[6] Inger Hee Mabuza Mathiesen,[4] Alexandra Gabriella Gheorge,[7] Frederik Boëtius Hertz,[8] Tavs Qvist,[4] Marvin Whiteley,[3,9,10] Peter Østrup Jensen,[1,2] Thomas Bjarnsholt [1,2]

ABSTRACT

Background A basic paradigm of human infection is that acute bacterial disease is caused by fast growing planktonic bacteria while chronic infections are caused by slow-growing, aggregated bacteria, a phenomenon known as a biofilm. For lung infections, this paradigm has been thought to be supported by observations of how bacteria proliferate in well-established growth media in the laboratory—the gold standard of microbiology.

Objective To investigate the bacterial architecture in sputum from patients with acute and chronic lung infections.

Methods Advanced imaging technology was used for quantification and direct comparison of infection types on fresh sputum samples, thereby directly testing the acute versus chronic paradigm.

Results In this study, we compared the bacterial lifestyle (planktonic or biofilm), growth rate and inflammatory response of bacteria in freshly collected sputum (n=43) from patient groups presenting with acute or chronic lung infections. We found that both acute and chronic lung infections are dominated by biofilms (aggregates of bacteria within an extracellular matrix), although planktonic cells were observed in both sample types. Bacteria grew faster in sputum from acute infections, but these fast-growing bacteria were enriched in biofilms similar to the architecture thought to be reserved for chronic infections. Cellular inflammation in the lungs was also similar across patient groups, but systemic inflammatory markers were only elevated in acute infections.

Conclusions Our findings indicate that the current paradigm of equating planktonic with acute and biofilm with chronic infection needs to be revisited as the difference lies primarily in metabolic rates, not bacterial architecture.

Key messages

What is the key question?
⇒ Acute infections are attributed to the action of planktonic bacteria, whereas chronic infections are described as involving biofilms; however, this basic paradigm of bacterial special structure in pneumonia remains unclear.

What is the bottom line?
⇒ This study reveals that the difference between acute and chronic lung infections is not the presence and absence of biofilm aggregates, but that acute infections have higher metabolic activity.

Why read on?
⇒ This paper challenges a 40-year-old (1982) paradigm of how bacteria proliferate in acute versus chronic lung infection. Our data reveal that biofilm growth is not reserved for chronic infections such as cystic fibrosis, but also predominates in community-acquired pneumonia, evoking equal inflammation of the lung, but with higher bacterial growth rates in acute infection.

INTRODUCTION

In the planktonic form, bacteria appear as single cells, whereas in the sessile form, bacteria are organised into multicellular aggregates, commonly referred to as biofilm.[1] No complete consensus definition of a biofilm exists but clinically relevant biofilms are often defined as 'A coherent cluster of bacterial cells imbedded in a biopolymer matrix, which, compared with planktonic cells, shows increased tolerance to antimicrobials and resists the antimicrobial properties of the host defence'.[2] Bacteria can readily transition between planktonic and biofilm lifestyles, and this phenomenon has been studied extensively in vitro.[3–5] Growth in either the planktonic or biofilm lifestyle has significant consequences for bacterial phenotypes.[6] One of the most striking differences between in vitro grown planktonic and biofilm bacteria is antibiotic tolerance, in which biofilm bacteria exhibit increased survival on exposure to multiple classes of antimicrobials.[7,8] This enhanced resistance has been attributed to a number of bacterial functions, including slow growth, altered expression of antimicrobial resistance mechanisms and possible depletion aggregation.[9–11] Based on these in vitro data, acute infections are often attributed to the action of planktonic bacteria, since they are generally curable with antibiotics, whereas chronic infections are described as involving biofilms, as they are

recalcitrant to antibiotic therapies.[12 13] However, this basic paradigm has not been quantitatively tested in samples from human infection sites, primarily because of the difficulties in imaging the bacterial populations in these samples with high resolution.

To address this gap in knowledge, we directly tested the existing paradigm that acute human infections are caused by planktonic cells and chronic infections are caused by biofilms. This was accomplished by quantifying the bacterial lifestyle (planktonic or biofilm), the growth rate and the degree of inflammation in sputum samples from patients with acute community-acquired pneumonia (CAP) without known chronic lung disease, acute pneumonia in chronic obstructive pulmonary disease (COPD) and chronic infections in cystic fibrosis (CF). Our overall aim was to investigate similarities and differences in the bacterial architecture in sputum from patients with either acute (CAP and COPD) or chronic (CF) lung infections.

MATERIALS AND METHODS
Additional methods are presented as online supplemental material.

Study design, setting, population and data collection
Patients with suspected pneumonia were prospectively recruited from 1 September 2016 to 1 January 2019 from two hospitals in Denmark: CAP or COPD from Nordsjællands Hospital, Denmark, and patients with CF from the Copenhagen CF Centre at Rigshospitalet, Denmark. Inclusion criteria for patients admitted with CAP and COPD were ≥18 years of age and purulent expectoration and at least one of the following symptoms: cough, chest pain or fever (>38.3°C rectally or >37.8°C auricular). Inclusion criteria for patients with CF attending the outpatient clinic were ≥18 years of age and the presence of a chronic lung infection. In CF, chronic bacterial infection was defined as the presence of pathogens in the lower respiratory tract at each monthly culture for more than 6 months, or for a shorter time in the presence of increased antibody response to pathogens

(>2 precipitating antibodies, normal: 0–1).[14 15] Patients from all groups were excluded if they had received antibiotics within 7 days of inclusion, were not able to expectorate, were unwilling or unable to consent or were expected not to survive the next 72 hours (figure 1). Among patients with CAP, information on COPD was retrieved from patient files and included self-reported diagnosis. All patients with CF were included, even though all were treated with antibiotics as part of routine clinical care. Data on patient demography and comorbidities were obtained from a questionnaire given to participants on the day of inclusion. Same day paraclinical parameters were obtained from patient medical records. Data on prior antibiotic treatment and corticosteroid use were obtained from patient questionnaires and medical records.

Ex vivo patient samples
Expectorated sputum samples were obtained from patients with CAP, COPD and chronic CF infections. Sputum samples (n=43) were fixed immediately after expectoration in phosphate-buffered saline that contained 4% paraformaldehyde and were embedded in paraffin. The sputum volumes range from 0.5 mL to 1 mL. Sections of 4.0 μm and 30.0 μm were cut using a standard microtome and were fixed on glass slides. The slides were stored at 4°C pending further analysis.

Preparation, staining and microscopy of sputum specimens
Sputum specimens measuring 4.0 μm and 30.0 μm were prepared and stained with peptide nucleic acid fluorescent in situ hybridisation (PNA-FISH) probes and 4′,6-diamidino-2-phenylindole (DAPI), as described elsewhere.[16] A Texas Red-conjugated PNA-FISH probe specific for bacterial 16S rRNA (AdvanDx, USA) was used to stain all bacteria present in the sputum. Specimen slides were scanned using a confocal laser scanning microscope (CLSM) (Axio Imager.Z2, LSM 880, Zeiss, Germany) and the accompanying software (Zen V.2.1, Germany). All images were obtained through a 63×/1.4 oil objective running a combination
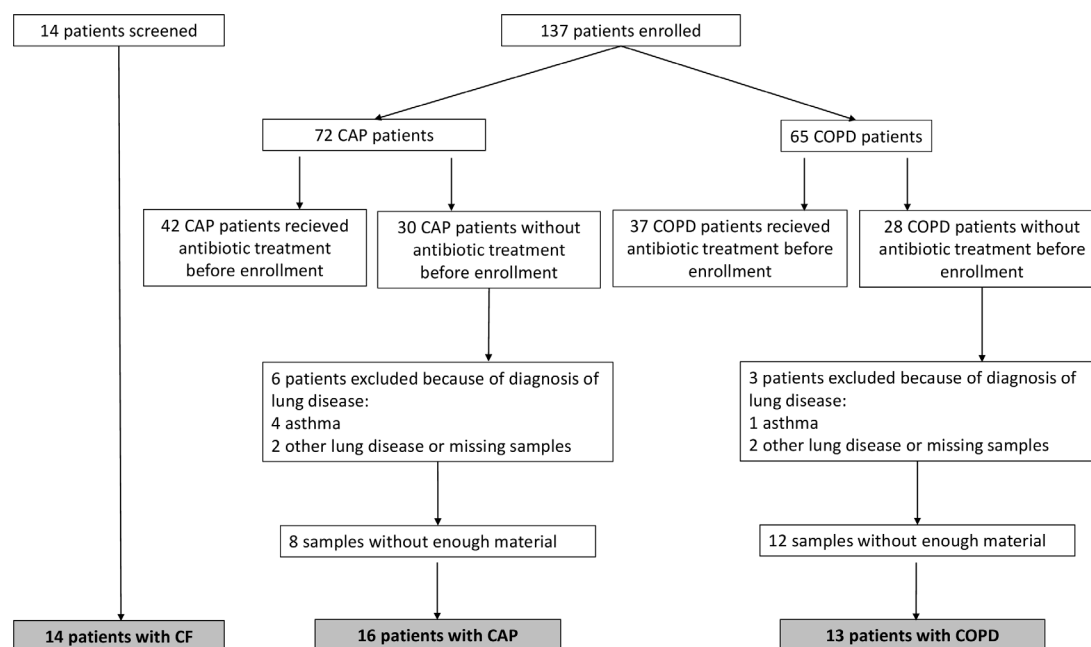
Figure 1 Flow chart of study and final diagnoses of patients recruited. The majority of patients screened and subsequently not recruited did not meet the requirements for untreated acute infection. CAP, community-acquired pneumonia; CF, cystic fibrosis; COPD, chronic obstructive pulmonary disease.

of two 405 nm and 594 nm lasers running in parallel tracks for excitation, with an emission range of 410–552 nm for DAPI and 602–686 nm for Texas Red. All images were obtained using identical levels of laser power and voltage on photodetectors (gain), respectively, for both tracks. A resolution of 2048×2048 pixels in the dimension of 134.95 (X)×134.95 (Y)×1.82 (Z), with Z-stack increments of 0.455 µm, was used for qualitative analysis. All pixels were scanned twice in an averaging mode at a colour depth of 16 bits.

For quantitative FISH and three-dimensional (3D) microscopy analysis, images of sputum specimens measuring 30.0 µm thick were obtained using a 7×7 tile scan with a 20% overlap between tiles. After tile stitching using a strict setting, the final images each measured 1304.0 (X)×1304.0 (Y)×52.65 (Z), with a resolution of 2320×2320 pixels and Z-stack increments of 0.351 µm. Each pixel was scanned twice in an averaging mode. Raw images were processed using Imaris V.8.2 (Bitplane, Switzerland). Objects ranging in size from 0.5 µm³ to 5.0 µm³ were classified as planktonic cells. Objects larger than 5.0µm³ were classified as aggregates, and objects smaller than 0.5µm³ were excluded from analysis.

Statistical methods
Statistical significance was evaluated using Student's t-test, Wilcoxon test, Kruskal-Wallis test and ordinary one-way analysis of variance, followed by Dunnett's or Bonferroni's multiple comparison test. A p value of ≤0·05 was considered statistically significant. Tests were performed using GraphPad Prism V.6.1 (GraphPad Software, La Jolla, California, USA) and Microsoft Excel (Microsoft Corp, Redmond, Washington, USA).

RESULTS
A total of 151 patients with CAP (n=72), COPD (n=65) and CF (n=14) were screened for inclusion. We excluded 79 patients because they had received antibiotic treatment within 7 days of enrolment, and 9 patients were excluded because they were diagnosed with chronic lung diseases other than COPD. In total, 43 patients (16 with CAP, 13 with COPD and 14 with CF) were included in our study (figure 1).

Baseline characteristics of patients
Patient characteristics on admission are described in table 1. Patients with CAP and COPD were older and had higher levels of C reactive protein than CF patients.

Microbiological findings
Potential causative bacterial pathogens were detected in 50% of patients with CAP, 46% of patients with COPD and 100% of patients with CF (see online supplemental tables 1 and 3). Bacteria identified in patients with acute infections included *Streptococcus pneumoniae*, *Haemophilus influenzae* and *Moraxella* sp, *Klebsiella* sp, *Pseudomonas aeruginosa* and *Staphylococcus aureus*. Finally, bacteria identified in patients with CF included *P. aeruginosa* (79%), *Achromobacter xylosoxidans*, *S. aureus*, *Mycobacterium abscessus*, *Klebsiella pneumoniae*, *Stenotrophomonas maltophilia* and *Burkholderia multivorans*. Virus detection was performed for patients with CAP and COPD using a nasopharyngeal swab or sputum sample (see online supplemental tables 2 and 4). Virus were detected in 50% of patients with CAP and among them 63% have co-infection with detected pathogens. In addition, virus was detected in two patients with COPD and only one have a co-infection.

Biofilms and single cells in all infection types
3D projections of biofilm and planktonic cells were obtained within CAP, COPD and CF sputum samples (figure 2A–C). These images revealed that the bacterial biomass within sputum samples from each infection type varied by at least 100-fold, although there was no difference in bacterial numbers between infection types (figure 2D). It was then determined whether the bacteria in each sputum sample were present as planktonic or aggregated cells. Planktonic cells were defined as those measuring 0·5–5·0 µm³, and cells in biofilm aggregates were defined as objects >5·0 µm³. All sample types contained both biofilm and planktonic cells, although on average, more bacterial biomass was present in biofilms than in planktonic cells (figure 2F). There were multiple samples within each type in which the biomass was dominated by biofilms (>90%), whereas only 2 CAP and 2 COPD samples had a planktonic cell biomass greater than 50%. There was a broad distribution of biofilm sizes in all samples, and 40 of the 43 samples had biofilms of at least 100 µm³ (figure 2E). In 19 samples (7 CAP, 5 COPD and 7 CF), more than 40% of the bacterial biomass was comprised of biofilms of 100 µm³ or larger.

Growth estimates based on fluorescence in sputum samples
PNA-FISH has the added benefit of providing quantitative information regarding the number of ribosomes within a cell, which can be used as an indirect measurement of metabolic activity.[17] Confocal images enabled quantification of fluorescence from 3D images at the single-cell level, thus avoiding several of the inherent challenges of 2D analyses. The distribution of bacterial

---

Table 1 Characteristics of 43 patients with lower respiratory tract infection

	*CAP (n=16)	*COPD (n=13)	CF (n=14)
Median age (years) (IQR)†‡	78 (69–84)	69 (61–81)	37 (25–48)
Female, n (%)	6 (37.5)	5 (38.5)	4 (28.6)
Median body mass index (kg/m²) (IQR)	26 (24–29)	28.3 (23.7–29)	21.7 (20.8–26.7)
Median CRP (mg/L) on admission (IQR)†‡	43 (15–101)	20 (10–151.5)	3.5 (2–7)
Diabetes, n (%)	3 (18.8)	3 (23.1)	6 (42.9)
Median blood neutrophil count (10⁸/L) on admission (IQR)	6 (5–10)	7.7 (5.2–10.8)	5.7 (3.9–9.5)
Duration of chronic infection (years)	NA	NA	22.5 (6–38)

Data are presented as % (counts), unless otherwise indicated.
*Patients with CAP and COPD with enough material and without other lung diseases and antibiotic treatment before enrolment.
†P <0.05 CAP vs CF by one-way ANOVA test or Kruskal-Walis test.
‡P <0.05 CF vs COPD by one-way ANOVA test or Kruskal-Walis test.
ANOVA, analysis of variance; CAP, community-acquired pneumonia; CF, cystic fibrosis; COPD, chronic obstructive pulmonary disease; CRP, C reactive protein; NA, not available.
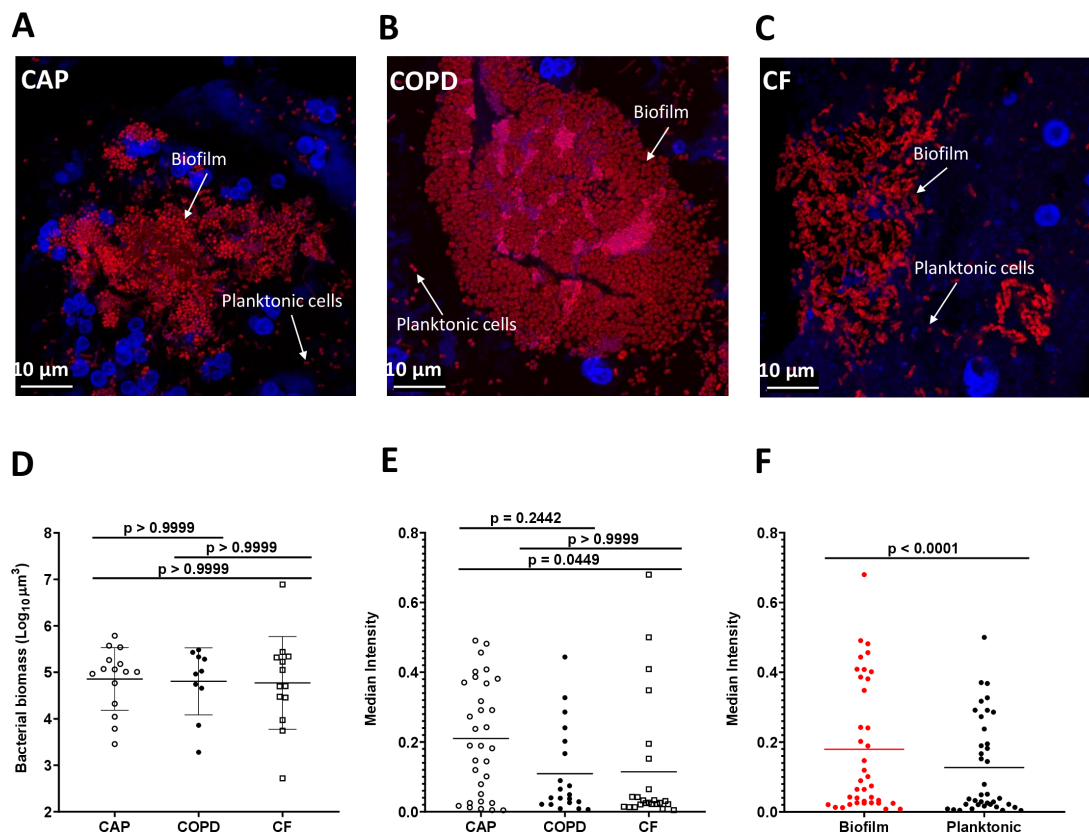
Figure 2 Biofilms and planktonic cells are observed across infection types. (A–C) Representative projections of confocal images of sputum samples of CAP with no detected pathogen (A), COPD with *Moraxella* sp (B) and CF with *Pseudomonas aeruginosa* (C). Specimens were stained with Tamra-5 (red) using PNA-FISH probes specific to bacterial 16S rRNA and DAPI m(blue). Scale bar is 10 μm. (D) Median total biomass of bacteria by infection type. Bacterial biomass was calculated on each sample (n=43) by counting the voxels representing bacteria after image analysis pipeline. There was no significant difference in sample biomass between infection types (p<0.05, Kruskal-Wallis test). (E) Comparing median sample intensity across infection type. Bacterial objects on each sample were identified, classified as either planktonic cells ($\leq 5\,\mu m^3$) or biofilms ($>5\,\mu m^3$) and their per cent contribution to total biomass was calculated. We found CAP samples to have the higher median intensity than CF samples (p<0.05, Kruskal-Wallis test), while COPD and CF samples, typically described chronic infections, have equivalent median intensity. (F) Comparing median sample intensity in biofilm (red) vs planktonic cells (black). We also found the median intensity of voxels in biofilms is higher than in planktonic cells (p<0.0001, Wilcoxon test). CAP, community-acquired pneumonia; CF, cystic fibrosis; COPD, chronic obstructive pulmonary disease; DAPI, 4′,6-diamidino-2-phenylindole; PNA-FISH, peptide nucleic acid fluorescent in situ hybridisation.

fluorescence intensities was examined, and the intensity that encompassed at least 50% of the bacterial population was calculated. The fluorescence intensity of bacterial cells in patients with CAP was significantly higher than that of bacterial cells in patients with CF and COPD, which indicates that populations in the CAP infecting bacteria had more ribosomes (figure 3A). In addition, biofilms in all sample types had significantly more cells at the maximum growth rate than planktonic cells (figure 3B). These results indicate that bacterial cells in patients with acute infections had more ribosomes, and thus higher metabolic activity, than those in patients with chronic lower respiratory tract infections (LRTIs). Additionally, the bacteria with higher ribosome numbers were enriched in biofilms than in planktonic cells in all sample types. The fluorescence intensity measurement from PNA-FISH staining in aggregates truly correlates with growth rate as there were no visible trends toward any form of dimming of mean fluorescence intensity units (FU) obtained from the biomass as the layers moved through the samples. Based on the quantified mean FU as a function of layer depth, linear regression with an F-test was used to assess if there was a dimming gradient from top to bottom of the FU. There was no significant slope in the regression based on the data, indicating

that there was no significant gradient through the layers of the 4-micrometre samples (sample 6, p=0.24; sample 21, p=0.06; and sample 45, p=0.18) (see online supplemental figure 3D-F). The same was valid for both the background signal and the signal from the DAPI-stained biomass, indicating no lost signal due to depth in the samples. In the nine 30-micrometre thick samples, the mean FU was quantified in each layer and in 3, three samples (9, 32 and 37) did not have a significant slope. Of the remaining six samples, only sample 6 had a significant negative slope with depth, indicating a loss of intensity as a function of depth. The other five samples had a positive slope meaning the regression increase with depth (see online supplemental figure 3G-O).

Based on the data in online supplemental figure 1D, we have estimated our study to be well powered, with 1-beta exceeding 0.943, for demonstrating a difference in FU between CF and CAP and between CF and COPD with p<0.05. However, the data indicate that our study was underpowered for finding a significant difference in FU between CAP and COPD with p<0.05.

Inflammatory cell distribution and degree of inflammation
Quantification of DAPI-stained inflammatory cells revealed no significant difference between inflammatory cell biomass in the
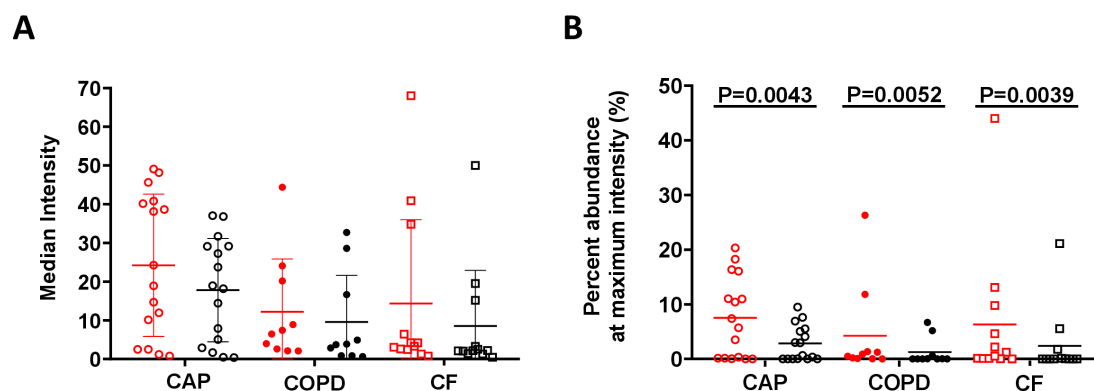
Figure 3 Estimation of bacterial growth rate based on fluorescence intensity. (A) The median intensity of bacterial voxels in biofilm (red) and planktonic (black) cells from infection types. We calculated the intensity emitted by biofilm and planktonic cells from each infection type and compared CAP infection samples with both COPD and CF samples. We found that CAP samples have higher intensity in both biofilm and planktonic cells than COPD (p=0.0356, Kruskal-Wallis test), suggesting that CAP infections have an increased growth rate compared with COPD and CF. (B) Per cent of bacterial population at maximum intensity. We calculated the portion of voxels at the highest fluorescence intensity value of biofilm (red) and planktonic (black) cells on each sample. We compared biofilms to planktonic cells within each infection type and found that biofilms have higher fluorescence intensity that planktonic cells in all infection types (p<0.01, unpaired Wilcoxon test). CAP, community-acquired pneumonia; CF, cystic fibrosis; COPD, chronic obstructive pulmonary disease.

three patient categories (see figure 4A). A custom analysis pipeline was used to evaluate the localisation of each inflammatory cell relative to the bacteria. This analysis revealed a proportional occupancy of inflammatory cells to bacterial cells, which quantitatively assessed the location of inflammatory cells in relation to bacterial cells compared with a null model in which the inflammatory cells were randomly positioned. This analysis found that inflammatory cells were not randomly distributed but were localised near bacteria, and the distance of the inflammatory cells from the bacteria was not statistically differentiated between the three patient categories (see figure 4B,C). In each sample type, the majority of inflammatory cells were localised within 2–3 microns of bacteria. These data indicate that sputum samples from patients with acute and chronic infections contained a range of inflammatory cells that were localised within microns of the bacteria.

To test if inflammation is a differentiating factor between chronic and acute infections, the degree of inflammation was assessed by blinded histopathological evaluation of all sputum samples. No significant difference in the degree of inflammation was identified between the three patient groups (see figure 4D).

DISCUSSION

The first study to describe the difference between acute and chronic infection was published by Marrie *et al*.[18] This study found that bacteria in blood were readily treatable with antibiotics, whereas bacteria in biofilm covering a pacemaker lead responded poorly to the same treatment.[18] Later, it was stated, 'But the fatal element in the biologically flawed strategy of acute pathogens was their adoption of the planktonic mode of growth'.[19] Microbiologists have since reasserted that acute infections are caused by planktonic bacteria, while chronic infections are caused by biofilm.[12] However, animal studies have shown that bacteria aggregate in acute wounds, as well as experimental blister wounds contain aggregates,[20 21] thus calling into question this paradigm.

A range of biofilm and planktonic bacteria were present in the sputum samples from both acute and chronic infections among individuals with and without chronic lung disease, although the biofilm phenotype predominated on average. All sputum samples contained biofilm, and only 5 of the 43 samples examined (2 CAP, 2 CF and 1 COPD) contained over 95% of bacteria in a single form (biofilm in each case). This finding indicates that biofilms and planktonic cells are generally present in the same sputum samples in both chronic and acute infections. This study's use of the classification 'planktonic' for objects 0·5 μm3–5·0 μm3 was conservative because this range of values could include small clusters of 2–4 cells. This classification was used because it lay within the range of known values for planktonic cells and thus accounted for potential impacts of environmental and physiological factors on bacterial size.[22]

A physical description of sputum bacteria as either planktonic cells or biofilm can be determined based on imaging to provide a direct test of the current paradigm. However, this assessment does not account for the phenotypes associated with planktonic cells and biofilm growth. For example, a biofilm that contain a low number of bacteria could be equally as susceptible to antibiotics as planktonic cells. Additionally, all bacteria observed were within sputum and not free swimming; therefore, the single cells bacteria observed in this study are not necessarily equivalent to the planktonic bacteria observed in in vitro shaken cultures. Recent data has showed that *P. aeruginosa* biofilms ~100·0 μm^3 exhibit increased resistance to phage and tolerance to aminoglycoside antibiotics; in the present study, 40 of the 43 samples had biofilms of this size or larger. Furthermore, in 19 samples (7 CAP, 5 COPD and 7 CF), more than 40% of the bacterial biomass was comprised of bacteria in biofilms of 100·0 μm^3 or larger. Therefore, sputum from both acute and chronic infections have biofilms of a volume that is known to be critical for antimicrobial tolerance, although acute infections are most often treatable with short courses of antibiotics.

There was no difference in the prevalence of planktonic and biofilm cells in acute and chronic LRTIs; however, the cells within acute CAP had increased numbers of ribosomes compared with COPD and CF. Ribosome numbers are associated with metabolic activity and are directly correlated with growth rates[17 23 24]; thus, bacteria in these acute infections are likely growing faster and have higher metabolic activity than bacteria in chronic infections. This finding may provide insight as to why acute infections frequently respond more adequately to antimicrobial treatment
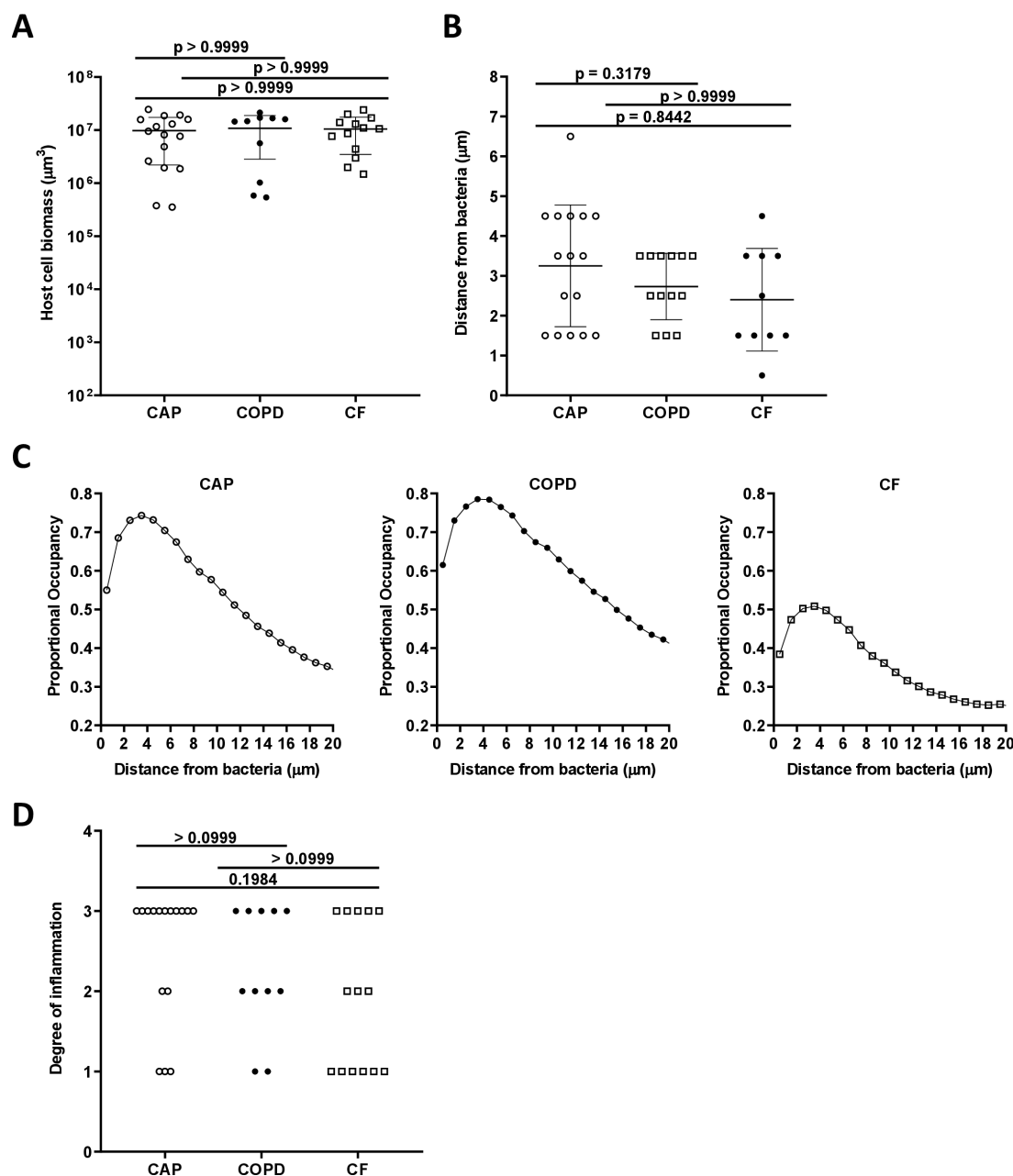
Figure 4 Host cell biomass in all infection types. (A) Mean total biomass of inflammatory cells by infection type. Confocal images of sectioned sputum were stained with DAPI and biomass calculated by the total number of and blue fluorescent voxels. (B) Distance from bacteria at which the proportional occupancy of inflammatory cells is highest for each sample type. (C) Proportional occupancy of inflammatory cells relative to bacteria. Representative samples of each type are shown: CAP (left), COPD (middle) and CF (right). Each point is the average value from 1000 random voxels in the image. (D) Blinded histopathological evaluation of sputum samples of degree of inflammation from sputum samples: from CAP (n=16), COPD (n=11) and CF (n=14). Degree of inflammation: 0: no inflammation, 1: mild inflammation, 2: moderate inflammation and 3: severe inflammation. Statistical significance was determined using (A) and (B) ordinary one-way ANOVA followed by Bonferroni multiple comparison test and (D) Kruskal-Wallis test (p≤0.05). ANOVA, analysis of variance; CAP, community-acquired pneumonia; CF, cystic fibrosis; COPD, chronic obstructive pulmonary disease; DAPI, 4′,6-diamidino-2-phenylindole

than chronic infections, because faster-growing bacteria are generally more susceptible to such treatment. To evaluate the impact of the depth of the bacterial biomass in the samples on the FU signal, we examined if FU signal was correlated with depth (online supplemental figure 3). No significant correlation in the 4-micrometre samples nor in the 30-micrometre samples was found, indicating the absence of significant influence of the depth of the bacterial biomass on the FU signal. The multiple peaks in the mean FU histogram may result from the z-axis positioning of the bacteria in the focal plane when several layers of bacteria are present, which is expected in clinical samples. Therefore, the FU signal was not corrected for the depth of the slides. However, although there was an overall difference in ribosome numbers between acute and chronic LRTIs, the differences were not consistent. For example, bacteria in two CF sputum samples contained the largest number of ribosomes of all the samples. Slow growth of *P. aeruginosa* and *S. aureus* within the chronic infected CF lung compared with in vitro

cultures has previously been presented but never correlated to acute infections.[17 25 26] As for the faster growth in the acute infections, we hypothesise that bacteria, as a default, grow as fast as possible only limited by the microenvironment. Therefore, they can grow exponentially in laboratory shaken cultures. Initially, when bacteria infect, they grow fast, evoke an inflammatory response as well as secrete virulence factors. This is also known from patients with CF, here the chronic infection is preceded by acute and intermittent infections.[27 28] Later, when the microenvironment changes with the pathological changes due to the inflammation, the growth declines as we show in this work.

Based on this, we hypothesise that the growth characteristics of the infecting bacteria are likely transient and affected by several factors. This is also evident from previous studies of CF lung infections showing great clonal diversity within different locations of the conductive airways, the clonal development likely depends on the microenvironment.[29] Future research could test this hypothesis by accessing data from longitudinal samples in the context of patient metadata. The results may also be translatable to other infection types; however, similar analyses should be performed in these patient cohorts. Furthermore, these results support the hypothesis that promoting bacterial growth in chronic infections may enhance the efficacy of antibiotics.[30 31]

Acute infections frequently generate a systemic immune response, whereas chronic infections generate a local and supposedly low-grade inflammatory response and are less likely to be eradicated.[13 17 32] This study found no detectable difference in the degree of inflammation or the numbers of inflammatory cells in acute and chronic sputum samples, which suggests that the resulting local inflammatory response was similar in both infection types. The inflammatory cells showed strong localisation to bacteria, which indicates that inflammatory cells were not impaired as expected but were able to identify and localise to bacteria within three microns in both acute and chronic infection samples.

Surprisingly, the testable hypothesis of planktonic versus biofilm infection has not previously been tested in a real-world setting of clinical disease. We did so with LRTI and found that biofilm infection is not only reserved for the chronic infection types but also predominates in acute infections such as CAP. Ultimately, the difference between the infecting bacteria in acute and chronic infections may come down to bacteria in acute infection having higher metabolic activity, leading to a greater systemic inflammatory response. The conceptual difference between infection types is thus in metabolic rate, not bacterial architecture. This would warrant a change in the understanding of chronic lung infections, redirecting focus to the metabolic state of the identified bacteria, rather than the presence or absence of biofilm bacteria and their matrix. It also has implications beyond lung infections as the finding represents a rejection of a central theory in bacteriology. Finally, the diagnostic criteria for chronic infections must be reassessed and should focus on the metabolic state of bacteria rather than aggregation of bacteria (biofilm) and their matrix.

This study focused on lung infections; however, the results may be translatable to other infection types; however, similar analyses should be performed in these patient cohorts.

Some bacterial species are typical pathogens of patients with COPD, why there can be a risk that patients may be undiagnosed for COPD. Underdiagnosis of COPD is a well-known global problem and Denmark is not exempt from this.[33] The validity of COPD coding practice in the hospital setting in Denmark has previously been assessed and reported by Lange *et al*[34]

documenting that the vast majority of outpatients with COPD diagnosis indeed have COPD, but that underdiagnosis remains a problem. Ideally, we could have performed lung function testing following admission in all the study patients, but this was not feasible. The study was performed in a clinical setting, and it is possible that misclassification of persons with an obstructive airway disease could introduce a bias. However, it is probable that there is still broad generalisability of our results, as these same biases are likely to exist in similar CAP-defined groups in other settings.

Author affiliations
[1]Department of Clinical Microbiology, Rigshospitalet, Copenhagen, Denmark
[2]Costerton Biofilm Center, Department of Immunology and Microbiology, University of Copenhagen Faculty of Health and Medical Sciences, Copenhagen, Denmark
[3]School of Biological Sciences, Georgia Institute of Technology, Atlanta, Georgia, USA
[4]Department of Infectious Diseases, Rigshospitalet, Copenhagen, Denmark
[5]Department of Pulmonary and Infectious Diseases, Nordsjællands University Hospital, Hillerød, Denmark
[6]Department of Medicine Section for Infectious Diseases, Herlev-Gentofte University Hospital, Hellerup, Denmark
[7]Department of Forensic Pathology and Forensic Medicine, Faculty of Health and Medical Sciences, University of Copenhagen, Copenhagen, Denmark
[8]Department of Clinical Microbiology, Herlev Hospital, Herlev, Denmark
[9]Emory-Children's Cystic Fibrosis Center, Atlanta, Georgia, USA
[10]Center for Microbial Dynamics and Infection, Georgia Institute of Technology, Atlanta, Georgia, USA

ORCID iDs
Mette Kolpen http://orcid.org/0000-0001-5575-0384
Thomas Bjarnsholt http://orcid.org/0000-0002-8003-7414

REFERENCES

1 Høiby N, Bjarnsholt T, Moser C, *et al*. ESCMID guideline for the diagnosis and treatment of biofilm infections 2014. *Clin Microbiol Infect* 2015;21 Suppl 1:S1–25.
2 Burmølle M, Thomsen TR, Fazli M, *et al*. Biofilms in chronic infections - a matter of opportunity - monospecies biofilms in multispecies infections. *FEMS Immunol Med Microbiol* 2010;59:324–36.
3 Sauer K, Camper AK, Ehrlich GD, *et al*. *Pseudomonas aeruginosa* displays multiple phenotypes during development as a biofilm. *J Bacteriol* 2002;184:1140–54.
4 Pamp SJ, Sternberg C, Tolker-Nielsen T. Insight into the microbial multicellular lifestyle via flow-cell technology and confocal microscopy. *Cytometry A* 2009;75:90–103.
5 Klausen M, Heydorn A, Ragas P, *et al*. Biofilm formation by *Pseudomonas aeruginosa* wild type, flagella and type IV pili mutants. *Mol Microbiol* 2003;48:1511–24.
6 Valli RXE, Lyng M, Kirkpatrick CL. There is no hiding if you Seq: recent breakthroughs in *Pseudomonas aeruginosa* research revealed by genomic and transcriptomic next-generation sequencing. *J Med Microbiol* 2020;69:162–75.
7 Stewart PS. Theoretical aspects of antibiotic diffusion into microbial biofilms. *Antimicrob Agents Chemother* 1996;40:2517–22.
8 Kim J, Hahn J-S, Franklin MJ, *et al*. Tolerance of dormant and active cells in *Pseudomonas aeruginosa* PA01 biofilm to antimicrobial agents. *J Antimicrob Chemother* 2009;63:129–35.
9 Brochmann RP, Toft A, Ciofu O, *et al*. Bactericidal effect of colistin on planktonic *Pseudomonas aeruginosa* is independent of hydroxyl radical formation. *Int J Antimicrob Agents* 2014;43:140–7.
10 Kolpen M, Kragh KN, Bjarnsholt T, *et al*. Denitrification by cystic fibrosis pathogens - *Stenotrophomonas maltophilia* is dormant in sputum. *Int J Med Microbiol* 2015;305:1–10.
11 Secor PR, Michaels LA, Ratjen A, *et al*. Entropically driven aggregation of bacteria by host polymers promotes antibiotic tolerance in *Pseudomonas aeruginosa*. *Proc Natl Acad Sci U S A* 2018;115:10780–5.
12 Bjarnsholt T, Ciofu O, Molin S, *et al*. Applying insights from biofilm biology to drug development - can a new approach be developed? *Nat Rev Drug Discov* 2013;12:791–808.
13 Bjarnsholt T. The role of bacterial biofilms in chronic infections. *APMIS Suppl* 2013;136:1–58.
14 Pressler T, Karpati F, Granström M, *et al*. Diagnostic significance of measurements of specific IgG antibodies to *Pseudomonas aeruginosa* by three different serological methods. *J Cyst Fibros* 2009;8:37–42.
15 Proesmans M, Balinska-Miskiewicz W, Dupont L, *et al*. Evaluating the "Leeds criteria" for *Pseudomonas aeruginosa* infection in a cystic fibrosis centre. *Eur Respir J* 2006;27:937–43.
16 Ring HC, Bay L, Nilsson M, *et al*. Bacterial biofilm in chronic lesions of hidradenitis suppurativa. *Br J Dermatol* 2017;176:993–1000.
17 Kragh KN, Alhede M, Jensen Peter Ø, *et al*. Polymorphonuclear leukocytes restrict growth of *Pseudomonas aeruginosa* in the lungs of cystic fibrosis patients. *Infect Immun* 2014;82:4477–86.
18 Marrie TJ, Nelligan J, Costerton JW. A scanning and transmission electron microscopic study of an infected endocardial pacemaker lead. *Circulation* 1982;66:1339–41.
19 Costerton JW. *The biofilm primer*. New York: Springer, 2007.
20 Bay L, Kragh KN, Eickhardt SR, *et al*. Bacterial aggregates establish at the edges of acute epidermal wounds. *Adv Wound Care* 2018;7:105–13.
21 Schaber JA, Triffo WJ, Suh SJ, *et al*. *Pseudomonas aeruginosa* forms biofilms in acute infection independent of cell-to-cell signaling. *Infect Immun* 2007;75:3715–21.
22 Levin PA, Angert ER. Small but mighty: cell size and bacteria. *Cold Spring Harb Perspect Biol* 2015;7:a019216.
23 Schaechter M, Maaloe O, Kjeldgaard NO. Dependency on medium and temperature of cell size and chemical composition during balanced grown of *Salmonella typhimurium*. *J Gen Microbiol* 1958;19:592–606.
24 Yang L, Haagensen JAJ, Jelsbak L, *et al*. In situ growth rates and biofilm development of *Pseudomonas aeruginosa* populations in chronic lung infections. *J Bacteriol* 2008;190:2767–76.
25 DePas WH, Starwalt-Lee R, Van Sambeek L, *et al*. Exposing the three-dimensional biogeography and metabolic states of pathogens in cystic fibrosis sputum via hydrogel embedding, clearing, and rRNA labeling. *mBio* 2016;7. doi:10.1128/mBio.00796-16. [Epub ahead of print: 27 Sep 2016].
26 Kopf SH, Sessions AL, Cowley ES, *et al*. Trace incorporation of heavy water reveals slow and heterogeneous pathogen growth rates in cystic fibrosis sputum. *Proc Natl Acad Sci U S A* 2016;113:E110–6.
27 Hansen CR, Pressler T, Høiby N. Early aggressive eradication therapy for intermittent *Pseudomonas aeruginosa* airway colonization in cystic fibrosis patients: 15 years experience. *J Cyst Fibros* 2008;7:523–30.
28 Bjarnsholt T, Jensen Peter Østrup, Fiandaca MJ, *et al*. *Pseudomonas aeruginosa* biofilms in the respiratory tract of cystic fibrosis patients. *Pediatr Pulmonol* 2009;44:547–58.
29 Jorth P, Staudinger BJ, Wu X, *et al*. Regional isolation drives bacterial diversification within cystic fibrosis lungs. *Cell Host Microbe* 2015;18:307–19.
30 Kolpen M, Lerche CJ, Kragh KN, *et al*. Hyperbaric Oxygen Sensitizes Anoxic *Pseudomonas aeruginosa* Biofilm to Ciprofloxacin. *Antimicrob Agents Chemother* 2017;61. doi:10.1128/AAC.01024-17. [Epub ahead of print: 24 Oct 2017].
31 PØ J, Kolpen M, Kragh KN. Micro-environmental characteristics and physiology of biofilms in chronic infections of CF patients are strongly affected by the host immune response. *APMIS* 2017.
32 Høgsberg T, Bjarnsholt T, Thomsen JS, *et al*. Success rate of split-thickness skin grafting of chronic venous leg ulcers depends on the presence of *Pseudomonas aeruginosa*: a retrospective study. *PLoS One* 2011;6:e20492.
33 Thomsen RW, Lange P, Hellquist B, *et al*. Validity and underrecording of diagnosis of COPD in the Danish national patient registry. *Respir Med* 2011;105:1063–8.
34 Lange P, Tøttenborg SS, Sorknæs AD, *et al*. Danish register of chronic obstructive pulmonary disease. *Clin Epidemiol* 2016;8:673–8.

Supplemental material

BMJ Publishing Group Limited (BMJ) disclaims all liability and responsibility arising from any reliance
placed on this supplemental material which has been supplied by the author(s)

Thorax

Supplemental table 1. Detected pathogens in sputum from 29 patients admitted with acute respiratory tract infection and 14 CF patients with chronic infection.			
	CAP (n=16)	**COPD (n=13)**	**CF (n=14)**
Negative sputum, n (%)	8 (50.0)	7 (53.8)	0 (0)
Positive sputum, n (%)	8 (50.0)	6 (46.2)	14 (100.0)
S. pneumonia, n (%)	3 (18.8)	1 (7.7)	0 (0)
H. influenza, n (%)	1 (6.3)	3 (23.1)	0 (0)
Moraxella sp. , n (%)	2 (12.5)	1 (7.7)	0 (0)
Mycoplasma sp. , n (%)	0 (0)	0 (0)	0 (0)
N. meningiditis, n (%)	1 (6.3)	0 (0)	0 (0)
Klebsiella sp. , n (%)	0 (0)	1 (7.7)	0 (0)
P. aeruginosa non mucoid, n (%)	0 (0)	1 (7.7)	9 (64.3)
P. aeruginosa mucoid, n (%)	0 (0)	0 (0)	6 (42.9)
A. xyloxosidans, n (%)	0 (0)	0 (0)	1 (7.1)
S. aureus, n (%)	0 (0)	1 (7.7)	2 (14.3)
M. abscessus, n (%)	0 (0)	0 (0)	1 (7.1)
K. pneumoniae, n (%)	0 (0)	0 (0)	1 (7.1)
S. maltophilia, n (%)	0 (0)	0 (0)	1 (7.1)
B. multivorans, n (%)	0 (0)	0 (0)	2 (14.3)
Mold, n (%)	0 (0)	0 (0)	5 (35.7)

Supplemental table 2. Detected virus in sputum from 29 patients admitted with acute respiratory tract infection.			
	CAP (n=16)	COPD (n=13)	CF (n=14)
Negative nasopharyngeal swap/sputum, n (%)	8 (50.0)	7 (53.8)	NA
Positive nasopharyngeal swap/sputum, n (%)	8 (50.0)	6 (46.2)	NA
Respiratory synctial virus RSV, n (%)	3 (18.8)	1 (7.7)	NA
Influenza A, n (%)	1 (6.3)	3 (23.1)	NA
Influenza B, n (%)	2 (12.5)	1 (7.7)	NA
Coronavirus, n (%)	0 (0)	0 (0)	NA
Rhinovirus/Enterovirus, n (%)	1 (6.3)	0 (0)	NA
Human metapneumovirus, n (%)	0 (0)	1 (7.7)	NA

Supplemental material

BMJ Publishing Group Limited (BMJ) disclaims all liability and responsibility arising from any reliance placed on this supplemental material which has been supplied by the author(s)

Thorax

Supplemental table 3. Observed and detected pathogens in biofilms and as planktonic cells in sputum from from 29 patients admitted with acute respiratory tract infection and 14 CF patients with chronic infection.

Group	No.	Patient ID	Observed biofilm	Observed single cells	No detected pathogen in sputum	Detected pathogen in sputum	S. pneumonia	H. Influenza	Moraxella sp.	Mycoplasma sp.	N. meningiditis	Klebsiella sp.	P. aeruginosa non mucoid	P. aeruginosa mucoid	A. xylosoxidans	S. aureus	M. abscessus	K. pneumoniae	S. Maltophilia	B. multivorans	Mold
CAP	2	008			X																
	4	057	X	X	X																
	6	062	X	X	X																
	8	064	X	X		X			X												
	10	069	X	X	X																
	12	079			X																
	14	087	X	X		X	X														
	16	089	X	X		X		X													
	20	106	X	X	X																
	22	110	X	X		X															
	24	114	X	X	X																
	26	120	X	X		X			X												
	28	128	X	X		X	X														
	29	129	X	X		X	X														
	30	131	X	X	X																
	31	132	X	X		X					X										
COPD	32	136	X	X		X						X	X								
	33	140	X	X		X			X												
	34	100	X	X		X	X		X												
	35	103			X																
	36	092	X	X	X																
	37	094			X																
	38	137	X	X	X																
	39	013	X	X	X																
	40	122	X	X		X										X					
	41	123		X	X																
	42	090	X	X		X		X													
	45	085	X	X		X			X												
	47	107	X	X	x																

Supplemental material

BMJ Publishing Group Limited (BMJ) disclaims all liability and responsibility arising from any reliance
placed on this supplemental material which has been supplied by the author(s)

Thorax

Supplemental table 3 (Continued). Observed and detected pathogens in biofilms and as planktonic cells in sputum from from 29 patients admitted with acute respiratory tract infection and 14 CF patients with chronic infection.

	Patient ID		Observed biofilm	Observed single cells	No detected pathogen in sputum	Detected pathogen in sputum	*S. pneumonia*	*H. Influenza*	*Moraxella sp.*	*Mycoplasma sp.*	*N. meningiditis*	*Klebsiella sp.*	*P. aeruginosa non mucoid*	*P. aeruginosa mucoid*	*A. xylosoxidans*	*S. aureus*	*M. abscessus*	*K. pneumoniae*	*S. Maltophilia*	*B. multivorans*	Mold
CF	1	17	X	X									X	X							
	3	59	X	X									X	X							
	5	63	X	X									X	X							X
	9	273	X	X									X								
	11	301	X	X									X			X					X
	13	355	X	X										X							
	15	396	X	X											X		X	X			
	17	408	X	X									X						X		X
	19	452	X	X												X				X	
	21	499	X	X									X	X							
	23	221		X									X								X
	48	264											X								
	49	286	X	X										X							X
	50	413	X	X																X	

Supplemental material

BMJ Publishing Group Limited (BMJ) disclaims all liability and responsibility arising from any reliance placed on this supplemental material which has been supplied by the author(s)

Thorax

	Patient ID		Virus	Negative nasopharyngeal swap/sputum	Positive nasopharyngeal swap/sputum	*Respiratory synctial virus, RSV*	*Influenza A*	*Influenza B*	*Coronavirus*	*Rhinovirus/Enterovirus*	*Human metapneumovirus*
Supplemental table 4. Detected virus in sputum from 29 patients admitted with respiratory tract infection											
CAP	2	008		X							
	4	057			X	X					
	6	062		X							
	8	064		X							
	10	069		X							
	12	079		X							
	14	087			X	X					
	16	089			X		X				
	20	106			X			X			
	22	110		X							
	24	114			X					X	
	26	120			X			X			
	28	128			X			X			
	29	129			X	X					
	30	131		X							
	31	132		X							
COPD	32	136		X							
	33	140		X							
	34	100			X					X	
	35	103		X							
	36	092		X							
	37	094		X							
	38	137		X							
	39	013		X							
	40	122		X							
	41	123		X							
	42	090		X							
	45	085		X							
	47	107			X						X

Supplemental material

BMJ Publishing Group Limited (BMJ) disclaims all liability and responsibility arising from any reliance
placed on this supplemental material which has been supplied by the author(s)

Thorax

	Chocolate blood *agar plates*(CBA)[a] (CO$_2$, 35ºC)	Blood *agar plates* (BA)[b] (CO$_2$, 35ºC)	Solid lactose agar plates ('Blue plates)[c] (35ºC)	Resistance agar plates[d] (35ºC)	Sabouraud agar plates[e] (37ºC)	NaCl[f] (35ºC)	BCSA agar plates[g] (CO$_2$, 35ºC)
Supplemental table 5: Diagnostic procedure of expectorated material from the lower respiratory tract of patients with or without pneumonia.							
Standard diagnostic	1 day	1 day	1 day				
Extended diagnostic	1-3 days	1-3 days	1-3 days	1-3 days	1-5 days	1-2 days	1-3 days

[a]**Chocolate blood agar plates (CBA):** (36.0 g L^{-1} GC Agar Base (15 g L^{-1} Peptone, 1.0 g L^{-1} Corn Starch, 4 g L^{-1} Dipotassium phosphate, 1 g L^{-1} Monopotassium phosphate, 5 g L^{-1} Sodium chloride, 10 g L^{-1} agar), 10.0 g L^{-1} Iso Vitalex Enrichment, 10.0 g L^{-1} Hemoglobin) (SSI)
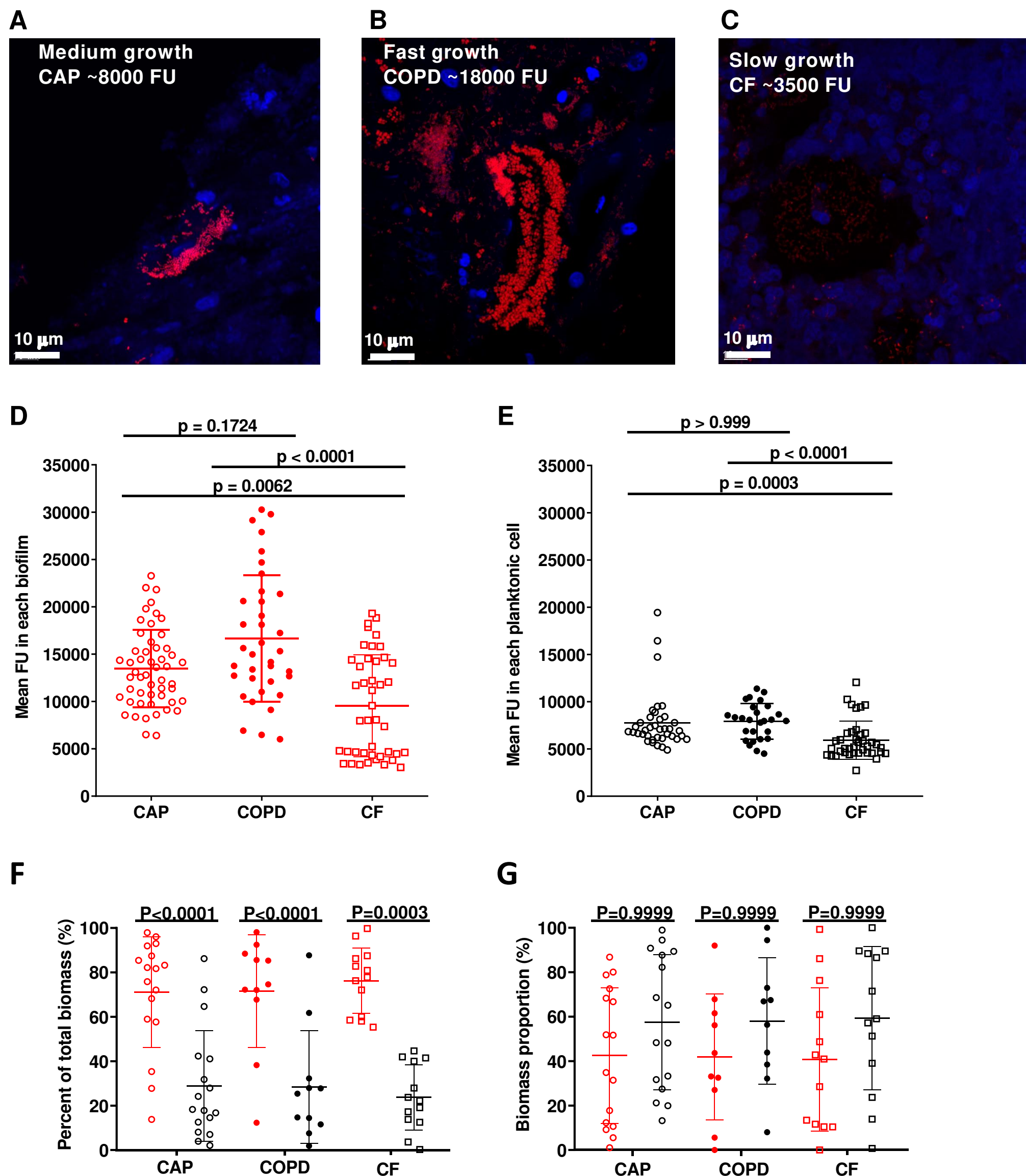
[b]**Blood *agar plates* (BA):**

[c]**Solid lactose agar plates ('Blue plates):** A modified Conradi-Drigalskimedium containing 10 g/L detergent, 1 g/L Na2S2O3·H2O, 0.1 g/L bromothymol blue, 9 g/L lactose and 0.4 g/L glucose, pH 8.0; (SSI)
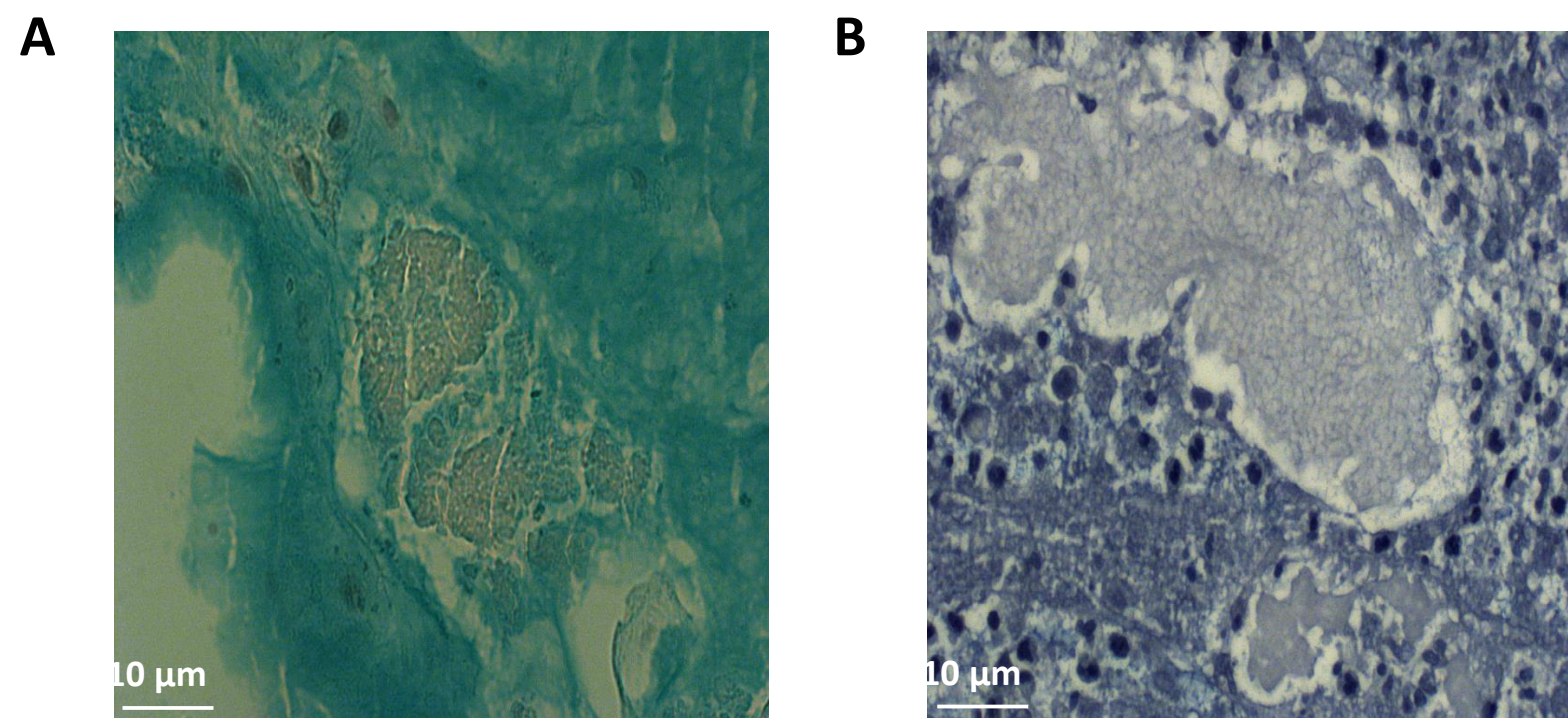
[d]**Resistance agar plates:**

[e]**Sabouraud agar plates:**

[f]**NaCl:**

[g]**BCSA agar plates:**

Supplemental material

BMJ Publishing Group Limited (BMJ) disclaims all liability and responsibility arising from any reliance placed on this supplemental material which has been supplied by the author(s)

Thorax

Supplemental figure 1. Fluorescence intensity in sputum samples. (A-C) Visualization of representative sputum samples from two CF patients and one CAP patient analysed with quantitative PNA-FISH based on fluorescence emitted from a universal bacteria specific PNA-FISH probe (16S rRNA). (A) CF sputum sample with non-growing or slow-growing cells based on the reduced numbers of intracellular ribosomal content (~3500 FU). (B) CF sputum sample with medium growing cells based on the numbers of intracellular ribosomal content (~8000 FU). (C) CAP sputum sample with fast growing cells based on the increased numbers of ribosomal content (~20500 FU). (D) Fluorescence intensity (FU) measured in each biofilm detected in images from sputum samples from CAP (n= 15), CF (n= 12) and COPD (n= 10). (E) Fluorescence intensity (FU) measured in all planktonic cells detected in images from sputum samples from CAP (n= 14), CF (n= 13) and COPD (n= 11). (F) Percent of total biomass in biofilms (red) and planktonic cells (black). (G) Proportion of biomass in biofilms (red) and planktonic cells (black). Statistical significance was determined using Kruskal-Wallis test (P≤0.05).

Supplemental material

BMJ Publishing Group Limited (BMJ) disclaims all liability and responsibility arising from any reliance
placed on this supplemental material which has been supplied by the author(s)

Thorax

A

B

10 µm

10 µm

Supplemental figure 2: Brightfield microscopy images of bacterial biofilms found in sputum samples from CAP patients. Samples were stained with Alcian Blue polysaccharide stain to visualize polysaccharide within the biofilms as part of the matrix. In both images, a visible scaffolding of stringy polysaccharide can be observed within the biofilms. The mucus surrounding the biofilms are highly stained as well as it contains large amounts of polysaccharide as well. In both images, several eukaryotic nuclei can be observed surrounding the biofilms, although in image B to a much higher degree. **(A)** This image was obtained with a color camera to display the blue staining. **(B)** This image was obtained using a mono-chrome camera which give high detains but in black and white display. 630x.

Supplemental figure 3: Test of fluoresces penetration in samples used for growth estimates based on PNA-FISH staining of rRNA. (A-C) three examples of the three investigated diagnosis. These three specimens were tested for fluorescent penetration. Results presented in D-F. D-F) Overlay graph of the mean FU measured in each of the 5 layers of the images (μm apart). The red bars represent the mean FU in the bacterial biomass. The blue bars represent the mean FU from the DAPI stained biomass. The gray bars represent the background fluorescence of the images. There was no significant slope gradient in any of the image. G-O) The mean FU histogram of nine randomly picked images, three from each investigated diagnose. The red bars represent the mean FU of the threshold bacterial biomass each layer of each images. The y-axis represent the depth in slides of the images.

Supplemental material:

Supplemental figure 1: **Fluorescence intensity in sputum samples.** (A-C) Visualization of representative sputum samples from two CF patients and one CAP-COPD patient analysed with quantitative PNA-FISH based on fluorescence emitted from a universal bacteria specific PNA-FISH probe (16S rRNA). (A) CF sputum sample with non-growing or slow-growing cells based on the reduced numbers of intracellular ribosomal content (~3500 FU). (B) CF sputum sample with medium growing cells based on the numbers of intracellular ribosomal content (~8000 FU). (C) CAP-COPD sputum sample with fast growing cells based on the increased numbers of ribosomal content (~20500 FU). (D) Fluorescence intensity (FU) measured in each biofilm detected in images from sputum samples from CAP-COPD (n= 15), CF (n= 12) and CAP+COPD (n= 10). (E) Fluorescence intensity (FU) measured in all planktonic cells detected in images from sputum samples from CAP-COPD (n= 14), CF (n= 13) and CAP+COPD (n= 11). (F) Percent of total biomass in biofilms (red) and planktonic cells (black). (G) Proportion of biomass in biofilms (red) and planktonic cells (black). Statistical significance was determined using Kruskal-Wallis test (P≤0.05).

Supplemental figure 2: **Brightfield microscopy images of bacterial biofilms found in sputum samples from CAP-COPD patients.** Samples were stained with Alcian Blue polysaccharide stain to visualize polysaccharide within the biofilms as part of the matrix. In both images, a visible scaffolding of stringy polysaccharide can be observed within the biofilms. The mucus surrounding the biofilms are highly stained as well as it contains large amounts of polysaccharide as well. In both images, several eukaryotic nuclei can be observed surrounding the biofilms, although in image B to a much higher degree. (A) This image was obtained with a colour camera to display the blue staining. (B) This image was obtained using a mono-chrome camera which give high detains but in black and white display. 630x.

Supplemental material

BMJ Publishing Group Limited (BMJ) disclaims all liability and responsibility arising from any reliance placed on this supplemental material which has been supplied by the author(s)

Thorax

Supplemental figure 3: Test of fluoresces penetration in samples used for growth estimates based on PNA-FISH staining of rRNA. (A-C) three examples of the three investigated diagnosis. These three specimens were tested for fluorescent penetration. Results presented in D-F. D-F) Overlay graph of the mean FU measured in each of the 5 layers of the images (µm apart). The red bars represent the mean FU in the bacterial biomass. The blue bars represent the mean FU from the DAPI stained biomass. The gray bars represent the background fluorescence of the images. There was no significant slope gradient in any of the image. G-O) The mean FU histogram of nine randomly picked images, three from each investigated diagnose. The red bars represent the mean FU of the threshold bacterial biomass each layer of each images. The y-axis represents the depth in slides of the images.

Supplemental methods:

Diagnostic procedure of collecting expectorated material from the lower respiratory tract of patients with or without pneumonia: Sputum samples were obtained for microbiological analysis and were processed according to standardized routine practices at the local microbiological departments. In brief, each sputum sample was analysed at either the Department of Clinical Microbiology at Herlev University Hospital (CAP) or Rigshospitalet (CF). Microbiological analysis included Gram-stain and microscopy to determine the quality of the sample. Respiratory pathogens were identified at Herlev Hospital using conventional culturing in air with 5% carbon dioxide (CO_2) at 35°C for 24 hours on 5% blood agar and chocolate agar plates (SSI Diagnostica, Denmark or Herlev Hospital). Samples were further analysed using culturing in ambient air at 35°C for 24 hours on blue agar plates with a modified Conradi-Drigalski diagnostic substrate selective for Gram-negative bacteria (SSI Diagnostica). Cultured species were identified using matrix-assisted laser desorption or ionization time-of-flight mass spectrometry (MALDI-TOF MS) (Bruker Daltonics, Billerica, MA, USA). Atypical bacteria (i.e., *Mycoplasma pneumoniae, Chlamydophila pneumoniae, Chlamydophila psittaci* and *Legionella pneumophila*) were identified using real-time polymerase chain reaction (PCR) (RotorGene Q and Qiasymphony, Qiagen, DSP virus or pathogen

Supplemental material

BMJ Publishing Group Limited (BMJ) disclaims all liability and responsibility arising from any reliance placed on this supplemental material which has been supplied by the author(s)

Thorax

mini kit, version 1 [Qiagen, kat.nr. 937036]), and respiratory viruses were also identified using PCR analysis (Influenza A, Influenza B and respiratory syncytial virus [RSV]) (Panther Fusion Assay, Hologic, Flu A/B/RSV Assay Cartridge). Extended culturing on both CF and CAP samples was performed at Rigshospitalet and used as a tool for research because it was relevant for CF patients, though perhaps excessive for CAP patients for routine diagnostics. The extended culturing included a Sabouraud plate for fungal growth, a 7% NaCl plate and a *Burkholderia cepacia* plate that contained colistin and gentamicin. The latter was used to identify bacteria with different susceptibility patterns and different colony morphologies. All cultures were assessed daily. All agar plates with positive cultures were processed according to routine practice. At the end of each day, one of two experienced laboratory technicians assessed the plates. Two colonies were stored in tubes with Mueller-Hinton broth plus 10% (vol/vol) glycerol at -80°C (see Supplemental Table 5).

Object identification

To identify objects, neighbouring voxels that shared at least one edge in the foreground were considered to be the same object. Objects ranging in size from $0.5–5.0$ μm^3 were classified as planktonic cells. Objects larger than 5.0 μm^3 aggregates were classified as aggregates, and objects smaller than 0.5 μm^3 were excluded from analysis. Total biomass was calculated by adding the volume of observations.

Quantitative PNA-FISH

The average fluorescence emitted by bacteria in either biofilms or planktonic cells was quantified as described with modifications using the freeware programme ImageJ (National Institutes of Health, USA). The foreground and background signals were defined by a threshold value, using the automated MultiThresholder macro for ImageJ to create a binary data set (K. Baler, G. Landini and W. Rasband, NIH, USA). Aggregates or regions with solely single cells were defined prior to measurement using the region of interest tool. The ImageJ function 'analyse particles' was used for quantification. The fluorescence intensity was calculated in fluorescence intensity units (FU) as the mean of grey-scale units over a range of $0–65,535$ FU. The average number of FUs emitted by the

Supplemental material

BMJ Publishing Group Limited (BMJ) disclaims all liability and responsibility arising from any reliance placed on this supplemental material which has been supplied by the author(s)

Thorax

PNA-FISH-treated cells was quantified for each sputum sample. We have previously validated the use of PNA FISH to estimate in vivo growth rates by demonstrating a significant ($P < 0.0001$) linear correlation between FU values and rRNA: number of rRNA molecules per rRNA gene molecule = 0.0447 x FU + 46.3 ($R^2 = 0.722$) [26].

To investigate if the depth of biomass affects the fluorescence units (FU) in samples stained with PNA-FISH, we quantified the mean FU of each layer within a biomass threshold in each image. Biomass foreground was defined with Otsu's method [36], and mean FU was reported with the use of FIJI [37]. The measurements were done on nine randomly picked of the samples sectioned to a thickness of 30 µm, three CAP, three COPD and three CF (see Supplemental Figure 3).

Image analysis

Images were analysed using a custom analysis pipeline (Matlab, Simulink) to distinguish between foreground and background. First, top and bottom boundaries were established for each sample by identifying terminal confocal sections that contained fluorescent voxels. The histograms of all slices on each image stack were combined and were then used to calculate a threshold for each channel using Otsu's method [36], resulting in the final threshold for the blue channel. Otsu-binarized images were then used to obtain final thresholds for the red channel. Foreground voxels on both channels were identified. The red channel intensity was collected from the raw images, and the minimum intensity of the top 1% of that population was used as the threshold for the red channel. Voxels in the final red images were subtracted from the blue channel to produce the final blue images.

Examination of sputum samples

To assess whether bacteria were present as planktonic cells or biofilm, sputum samples from all 43 patients were visualized using peptide nucleic acid fluorescent in situ hybridization (PNA-FISH). PNA-FISH uses fluorescently labelled probes specific to 16S ribosomal ribonucleic acid (rRNA) sequences to identify microbes and quantify the intracellular rRNA content. In this case, a universal bacterial PNA-FISH probe specific to 16S rRNA was used to visualize all bacteria, and samples

Supplemental material

BMJ Publishing Group Limited (BMJ) disclaims all liability and responsibility arising from any reliance
placed on this supplemental material which has been supplied by the author(s)

Thorax

were counterstained with the blue-fluorescent DNA stain 4',6-diamidino-2-phenylindole (DAPI) to
visualize eukaryotic cells. After staining, three-dimensional (3D) micrographs were obtained using
confocal laser scanning microscopy. One of the key challenges of this study was developing
methodology to identify fluorescently labelled bacteria in the presence of the high intrinsic
background fluorescence in the sputum samples. This was accomplished using a custom image
analysis pipeline to establish a background threshold fluorescence for each image.

Proportional occupancy

To determine proportional occupancy, binarized image stacks were analysed using a custom
pipeline developed in the programming language R. Briefly, a focal voxel in the 3D image was
selected at random, and the voxels of a specific channel located within a distance interval (radius 1
and radius 2) of the focal voxel were counted. This analysis revealed a proportional occupancy of
inflammatory cells to bacterial cells, which quantitatively assessed the location of inflammatory
cells in relation to bacterial cells compared to a null model in which the inflammatory cells were
randomly positioned. Proportional occupancy was then calculated by multiplying the number of
voxels within the distance range by the size of each voxel, then dividing that number by the total
volume of the distance interval.

$$Proportional\,Occupancy = \frac{number\,of\,voxels \in distance\,interval \times voxel\,volume}{total\,volume\,of\,interval}$$

Proportional occupancy was obtained for a representative amount of focus voxels per image,
starting from a distance of 1.0 μm away from each focal voxel and increasing by 1.0 μm distance
intervals up to 25.0 μm away from focus voxel. Proportional occupancy was calculated using
bacterial cells as a focal point and inflammatory cells as the surrounding environment, and it was
also calculated using inflammatory cells as a focal point and bacterial cells as the surrounding
environment.

Calculating community fluorescence intensity in aggregates and planktonic cells

The fluorescence intensity of each voxel—3D version of pixel—representing bacterial cells was
collected to capture the distribution fluorescence intensity across the bacterial community on each

Supplemental material

BMJ Publishing Group Limited (BMJ) disclaims all liability and responsibility arising from any reliance placed on this supplemental material which has been supplied by the author(s)

Thorax

sample. Each voxel was classified according to the size of the object they belong as either an aggregate or a planktonic cell and their intensity was normalized to range from zero to one. Bacterial voxels from planktonic cells and aggregates were then separately sorted based on normalized intensity and the minimum intensity at each population quartile was obtained. This analysis results in the identification of the range of intensities of specific percentages of bacterial communities, classified as aggregates or planktonic cells.

Additionally, the percentage of voxels at the maximum normalized intensity for aggregates and planktonic cells was calculated for each sample. The p-values for all pair-wise comparisons were calculated using unpaired Wilcoxon test.

Matrix staining: Alcian blue, lectins and eDNA

Sputum specimens measuring 4.0 µm thick were stained with Alcian blue (Merck, USA), according to the protocol by[38] used by Survarna et al. for extracellular polysaccharide for biofilm matrix components. The stained specimens were then evaluated using bright field microscopy on an Axio Imager.Z2 with Axiocam 305 camera (Zeiss, Germany). A pale blue stain surrounding dense aggregation of bacteria indicated the presence of polysaccharide (see Supplemental Figure 2).

Histopathology

For histopathological examination, sputum samples were immediately fixed in phosphate-buffered saline (PBS) with 4% paraformaldehyde and were maintained at 5°C prior to further preparation. The sputum samples were then embedded in paraffin. Samples were cut at 4.0 µm thickness, mounted in glass slides and stained with hematoxylin and eosin for the histological assessment.

Based on an overview at low magnification (62·5×) and detailed studies of five different areas of the sputum sample under high magnification (500×), the degree of inflammation was scored as 0 (no inflammation), 1 (mild inflammation), 2 (moderate inflammation) or 3 (severe inflammation with necrosis or severe inflammation throughout the sputum sample) [39]. The

histopathological assessment was completed blindly by a board-certified pathologist. Histopathological assessment was performed using a Laica DM 4000 B LED microscope.